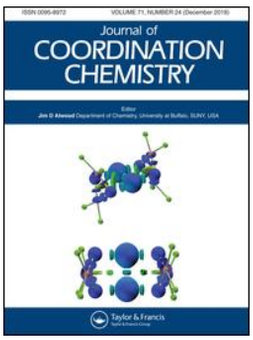

Journal of Coordination Chemistry

ISSN: 0095-8972 (Print) 1029-0389 (Online) Journal homepage: https://www.tandfonline.com/loi/gcoo20

Syntheses, structural characterization, DNA-cleavage and antioxidant features of the new tetra-substituted organo-soluble non-peripherally Co^{II}, Cu^{II}, Zn^{II} and Mg^{II} phthalocyanines

Halise Yalazan, Burak Barut, Gülpınar Sarkı, Beytullah Ertem, Yasemin Ünver, Arzu Özel & Halit Kantekin

To cite this article: Halise Yalazan, Burak Barut, Gülpınar Sarkı, Beytullah Ertem, Yasemin Ünver, Arzu Özel & Halit Kantekin (2019): Syntheses, structural characterization, DNA-cleavage and antioxidant features of the new tetra-substituted organo-soluble non-peripherally Co^{II}, Cu^{II}, Zn^{II} and Mg^{II} phthalocyanines, Journal of Coordination Chemistry, DOI: 10.1080/00958972.2019.1648795

To link to this article: https://doi.org/10.1080/00958972.2019.1648795

JOURNAL OF COORDINATION CHEMISTRY
https://doi.org/10.1080/00958972.2019.1648795

Syntheses, structural characterization, DNA-cleavage and antioxidant features of the new tetra-substituted organo-soluble non-peripherally Co^{II}, Cu^{II}, Zn^{II} and Mg^{II} phthalocyanines

Halise Yalazan[a], Burak Barut[b], Gülpınar Sarkı[a], Beytullah Ertem[c], Yasemin Ünver[a], Arzu Özel[b,d] and Halit Kantekin[a]

[a]Department of Chemistry, Karadeniz Technical University, Trabzon, Turkey; [b]Faculty of Pharmacy, Department of Biochemistry, Karadeniz Technical University, Trabzon, Turkey; [c]Vocational School of Health Services, Karadeniz Technical University, Trabzon, Turkey; [d]Drug and Pharmaceutical Technology Application and Research Center, Karadeniz Technical University, Trabzon, Turkey

ABSTRACT

This paper encompasses the synthesis, structural characterization, and evaluation of supercoiled pBR322 plasmid DNA-cleavage and DPPH (2,2-diphenyl-1-picrylhydrazyl) radical scavenging properties of newly synthesized tetra-substituted Co^{II} (**5**), Cu^{II} (**6**), Zn^{II} (**7**) and Mg^{II} (**8**) phthalocyanines bearing 4-methyl-*N*-(4-morpholinophenyl)benzenesulfonamide units at non-peripheral sites of phthalocyanine skeleton. The structural characterization of these new metallated phthalocyanines were performed *via* UV-vis, elemental analysis, FT-IR (ATR sampling accessory), ^{1}H-NMR and ^{13}C-NMR spectroscopic techniques (for **7** and **8**) and MALDI-TOF mass spectral data. The new compounds (**5**–**8**) exhibited good solubility in common organic solvents, and as well as no sort of aggregation was perceived at studied concentrations and solvents. Compound **7** indicated oxidative photocleavage activities in the presence of H_2O_2, indicating the conversion of supercoiled pBR322 plasmid DNA to nicked circular form (19.90%) and linear form (4.40%). Compound **5** displayed the highest radical scavenging activities among the tested compounds. The DPPH-radical scavenging percentages of **5** ranged from $85.35 \pm 2.45\%$ (12.5 μM) to $95.38 \pm 1.44\%$ (100 μM). These compounds are favorable for further research, owing to a broad range of biological and pharmaceutical activities of morpholine scaffold.

ARTICLE HISTORY
Received 23 April 2019
Accepted 12 July 2019

KEYWORDS
Cobalt(II) phthalocyanine; 4-morpholinoaniline; tosylation; plasmid DNA; antioxidant

CONTACT Beytullah Ertem bertem@ktu.edu.tr

Supplemental data for this article is available online at https://doi.org/10.1080/00958972.2019.1648795

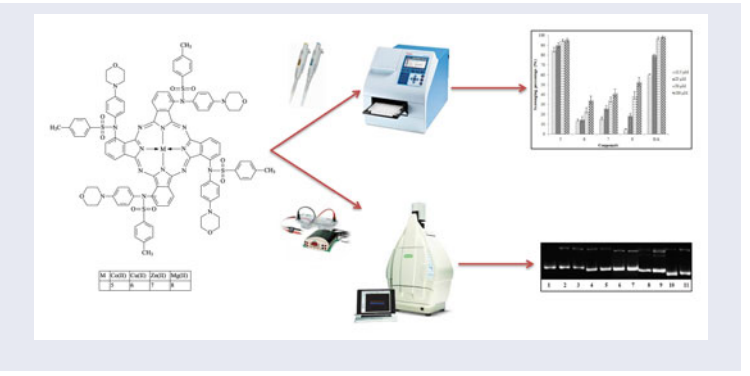

1. Introduction

Metallophthalocyanines (MPcs), which are metal-coordinated macrocycles of free-base phthalocyanines (Pcs), have been of great attraction for years due to their versatility and perfect features in terms of light, thermal and chemical stability, genuine electrochemical [1], photophysical–chemical [2, 3] and catalytic performance [4], also as the spectacular metal-coordination characteristics [5–10]. Both Pcs and MPcs are utilized in the area of material science such as photosensitizing agents in photodynamic therapy of diverse cancer diseases [11–13], liquid crystals [14, 15], dyes [16], photovoltaics [17], gas sensors [18], nonlinear optical materials [19], electrochromic devices [20], dye-sensitized solar cells [21], Langmuir Blodgett films [22], enzyme inhibition [23] and fluorescence "off–on–off" sensor [24]. Owing to their intense colors, MPcs have been great materials especially for the production of dyes and pigments for a long time. The total production of MPcs is nearly 80,000 tones throughout the world and its total manufacturing cost price is over one billion U.S. dollars [25, 26]. The solubility of the phthalocyanine compounds plays a critical role to evaluate these synthetic aromatic heterocycles in the field of material science summarized above. Another critical factor to employ these products in the above-mentioned applications is to prevent the aggregation of Pcs or MPcs, which is formed by π–π stacking interactions of Pc rings.

By the incorporation of four 4-methyl-*N*-(4-morpholinophenyl)benzenesulfonamide moieties into the non-peripheral positions of phthalocyanine skeleton, we obtained new tetra-substituted non-peripheral MPcs, which are carrying the morpholine and tosylated tertiary aromatic amine functionalities on the same molecular structure. As it is well known, morpholine moiety has nitrogen and oxygen atoms inside a heterocyclic six-membered ring and its numerous derivatives are utilized in diverse pharmaceutical and biological applications comprising antimalarial, antidepressant, antitumor, HIV-protease inhibitors, antiparasitic, antiinflammatory, local anesthetic, anticancer, analgesic, antifungal, appetite suppressant, selective inhibition of protein kinase C, antituberculosis and hypolipidemic activities [27–32]. Morpholine scaffold is also a useful starting compound and extensively used in organic synthesis as well [33].

It is well-known that DNA is the crucial target in the research and development of chemotherapeutic agents. The transition metal compounds as chemotherapeutic agents have increased in recent years due to their DNA-interaction properties. If these

agents interact with DNA, DNA-damage can occur in cancer cells and effects on cell proliferation and gene mutations that can trigger cell death [34].

As previously stated that the compounds carrying morpholine skeleton have the potential to be employed in biological and pharmaceutical applications, we designed a new study to examine the DNA-cleavage and antioxidant properties following the syntheses and structural verification of the new tetra-substituted phthalocyaninato cobalt(II) (**5**), copper(II) (**6**), zinc(II) (**7**) and magnesium(II) (**8**) compounds bearing 4-methyl-*N*-(4-morpholinophenyl)-benzenesulfonamide moieties at α-positions (non-peripheral sites) of the Pc core. Coupled with the results of DNA-cleavage and antioxidant properties, we found that zinc(II) Pc (**7**) has a potential utilization in the oxidative photocleavage and cobalt(II) (**5**) has remarkable radical scavenging activities.

2. Experimental

2.1. Chemicals and instrumentation

Instrumentation and materials as well as chemicals are provided as Supplementary Information. 3-Nitrophthalonitrile (**3**) was synthesized by the procedure cited [35].

2.2. DNA-cleavage studies

DNA-cleavage studies provided as Supplementary Information.

2.3. DPPH (2,2-diphenyl-1-picrylhydrazyl) radical scavenging assay

DPPH radical scavenging assay part provided as Supplementary Information.

2.4. Syntheses

2.4.1. 4-Methyl-N-(4-morpholinophenyl)benzenesulfonamide (2)

Under nitrogen atmosphere, 4-morpholinoaniline (**1**) (1.0 g, 5.61 mmol) was dissolved in dry pyridine (20 mL) inside a 50 mL round bottom flask and deaerated a couple of times. At −5 °C, *p*-toluenesulfonyl chloride (TsCl) (1.069 g, 5.61 mmol) in dry pyridine (10 mL) was dropwise added to the flask content within 30 min. When the dropwise addition of TsCl solution was over, a color change was observed in the reaction mixture from dark red-brownish to purple. Thereafter, the stirring continued under a nitrogen stream at −5 °C for 4 h and the stirring was maintained for one night at room temperature. Then, the reaction mixture was stirred during the addition of crushed ice (150 g) at room temperature for 3 h. Following that, concentrated HCl acid (54 mL) was added dropwise in 30 min to maintain the acidity of the mixture and subsequently, the aqueous solution extracted with chloroform (4 × 25 mL). The collected chloroform solvent over the aqueous layer was dried by the addition of anhydrous Na_2SO_4. The combined extract was vaporized by a rotary evaporator to remove chloroform to obtain **2** as a pale purple solid. Yield: 1.28 g (68.8%), m.p. 187–189 °C. Elemental analysis: Calc. (%) for $C_{17}H_{20}N_2O_3S$: C, 61.42; H, 6.06; N, 8.43; S, 9.65. Found: C, 60.47; H, 5.82; N, 8.58; S, 9.48. FT-IR: υ_{max} (cm^{-1}): 3154 (N–H), 3035 (C–H aromatic),

2967–2919–2900 (CH_3), 1599 (C=C), 1511, 1450, 1336–1158 (SO_2-tosyl group), 1263, 1239, 1115, 1090, 1051 (N–H), 918, 807, 738, 661. ^{1}H-NMR (δ in ppm, $CDCl_3$): 8.88 (s, 1H, N–*H*), 7.61–7.59 (d, 2H, Tosyl, Ar–*H*), 7.22–7.20 (d, 2H, Tosyl, Ar–*H*), 7.01–6.97 (d, 2H, Ar–*H*), 6.83–6.79 (d, 2H, Ar–*H*), 3.88–3.86 (t, 4H, O–CH_2), 3.13–3.11 (t, 4H, N–CH_2), 2.38 (s, 3H, CH_3). ^{13}C-NMR (δ in ppm, $CDCl_3$): 148.70, 148.43, 132.96, 129.01, 126.10, 110.52, 107.91, 107.39, 106.19, 105.91, 67.17–66.62–64.93 (O–CH_2), 50.12–49.83–49.65 (N–CH_2), 22.31–21.59–20.59 (Ar–CH_3). MALDI-TOF MS *m/z*: calculated: 332.42; found: 332.07 $[M]^+$.

2.4.2. N-*(2,3-Dicyanophenyl)-4-methyl*-N-*(4-morpholinophenyl)benzenesulfonamide (4)*

4-Methyl-*N*-(4-morpholinophenyl)benzenesulfonamide (**2**) (1.28 g, 3.98 mmol) and 3-nitrophtalonitrile (**3**) (0.69 g, 3.98 mmol) were dissolved in dry DMF (15 mL) in the Schlenk system. After efficient stirring 15 min at 55 °C, anhydrous K_2CO_3 (1.65 g, 12.00 mmol) was added to the solution by portion wise over 2 h and was degassed under the $N_{2(g)}$ flow. The reaction mixture was then heated at 55 °C for 138 h and completion of the reaction was monitored by thin layer chromatography (TLC). After completion of the reaction, the reaction mixture was cooled to room temperature and following the addition of crushed ice (200 g) and then stirred efficiently for 2 h at the same temperature. Later, the stirring mixture was filtered off and dried *in vacuo*. Subsequently, the dicyano derivative **4** was purified *via* crystallization using ethyl alcohol. After filtration, **4** was dried in a vacuum desiccator, following the washing with cold ethanol. Color: Light brown. Yield: 0.75 g (42.4%), m.p. 190–194 °C. Elemental analysis: Calc. (%) for $C_{25}H_{22}N_4O_3S$: C, 65.48; H, 4.84; N, 12.22; S, 6.99. Found (%): C, 64.94; H, 4.77; N, 11.96; S, 6.75. FT-IR, υ_{max} (cm^{-1}): 3073–3054 (Aromatic C–H), 2967–2920 (CH_3), 2233 (C≡N), 1583 (C = C), 1512, 1466, 1451, 1362–1165 (SO_2-tosyl group), 1281, 1239, 1123, 1089, 926, 820, 735, 668. ^{1}H-NMR (δ in ppm, $CDCl_3$): 7.94–7.89 (m, 2H, Tosyl, Ar–*H*), 7.73–7.65 (m, 2H, Tosyl, Ar–*H*), 7.32–7.21 (m, 3 H, Ar–*H*), 6.80–6.72 (m, 4H, Ar–*H*), 3.83–3.80 (t, 4H, O–CH_2), 3.17–3.15 (t, 4H, N–CH_2), 2.45 (s, 3H, CH_3). ^{13}C-NMR (δ in ppm, $CDCl_3$): 151.20, 145.73, 144.84, 135.45, 134.67, 133.76, 132.37, 130.47, 130.15, 129.80, 128.45, 117.89, 117.84, 115.40 (*C*≡N), 114.79, 113.58, 66.64–65.84 (O–CH_2), 48.29 (N–CH_2), 21.69 (Ar–CH_3). MALDI-TOF MS *m/z*: calculated: 458.53; found: 458.17 $[M]^+$.

2.4.3. Syntheses of non-peripherally metallophthalocyanines (5–8)

The dicyano derivative **4** (0.1 g, 0.218 mmol), anhydrous metal salts [$CoC1_2$ (14.15 mg, 0.109 mmol, for **5**); $CuCl_2$ (14.76 mg, 0.109 mmol, for **6**); $Zn(OAc)_2$ (20.00 mg, 0.109 mmol, for **7**); $MgC1_2$ (10.38 mg, 0.109 mmol, for **8**)], dry *n*-amyl alcohol (3.0 mL) and DBU {1,8-diazabicyclo[5.4.0]undec-7-ene} (catalytic amount was employed) were added into a standard Schlenk tube. Then, the content of the Schlenk tube was deaerated by the flow of inert $N_{2(g)}$ and heated at 160 °C for 17 h. As the content of the Schlenk tube was cooled to room temperature, ethanol (10 mL) was added to the green reaction mixture to maintain the precipitation of the synthesized compound and was stirred for 1 h. Subsequently, the precipitated crude compounds were filtered off and kept inside a vacuum desiccator until they were dried up. Finally, the

synthesized new metallated phthalocyanines (**5**–**8**) depurated by basic alumina-packed column chromatography with chloroform for **5** and **6** and chloroform:ethanol solvent mixture (50:2.5 v/v) for **7**, and (5:1 v/v) for **8**. The collected organic solvent mixture was removed by rotary evaporation and dried *in vacuo* to obtain the corresponding non-peripheral tetra-substituted metallophthalocyanines as dark (**5**, **6** and **7**) or light green (**8**) solids.

2.4.3.1. Non-peripherally phthalocyaninato cobalt(II) (5). Color: Dark green. Yield: 25.0 mg (24.2%), m.p. >300 °C. Elemental analysis: Calc. (%) for $C_{100}H_{88}N_{16}O_{12}S_4Co$: C, 63.45; H, 4.69; N, 11.84; S, 6.78. Found (%): C, 62.91; H, 4.57; N, 11.58; S, 6.39. FT-IR, υ_{max} (cm^{-1}): 3065 (Aromatic C–H), 2955–2917 (CH_3), 1602, 1507, 1478, 1449, 1351–1161 (SO_2–tosyl group), 1120, 1090, 928, 813, 761, 662. UV-vis ($CHC1_3$), λ_{max}, nm (logε): 327 (4.84), 607 (4.42) and 671 (5.01). MALDI-TOF MS *m/z*: calculated: 1893.07; found: 1893.23 $[M]^+$.

2.4.3.2. Non-peripherally phthalocyaninato copper(II) (6). Color: Dark green. Yield: 40.0 mg (38.6%), m.p. >300 °C. Elemental analysis: Calc. (%) for $C_{100}H_{88}N_{16}O_{12}S_4Cu$: C, 63.29; H, 4.67; N, 11.81; S, 6.76. Found (%): C, 62.45; H, 4.64; N, 11.56; S, 6.37. FT-IR, υ_{max} (cm^{-1}): 3065–3034 (Aromatic C–H), 2953–2919 (CH_3), 1600, 1508, 1449, 1352–1161 (SO_2–tosyl group), 1121, 1090, 928, 813, 764, 661. UV-vis ($CHC1_3$), λ_{max}, nm (logε): 344 (4.71), 612 (4.35) and 680 (5.01). MALDI-TOF MS *m/z*: calculated: 1897.68; found: 1897.11 $[M]^+$.

2.4.3.3. Non-peripherally phthalocyaninato zinc(II) (7). Color: Dark green. Yield: 41.0 mg (39.5%), m.p. >300 °C. Elemental analysis: Calc. (%) for $C_{100}H_{88}N_{16}O_{12}S_4Zn$: C, 63.23; H, 4.67; N, 11.80; S, 6.75. Found (%): C, 62.53; H, 4.62; N, 11.66; S, 6.44. FT-IR, υ_{max} (cm^{-1}): 3044 (Aromatic C–H), 2956–2920 (CH_3), 1606, 1509, 1488, 1449, 1332–1159 (SO_2–tosyl group), 1118, 1087, 926, 813, 762, 660. ^{1}H-NMR (δ in ppm, $CDCl_3$): 7.81–7.60 (m, 20H, Ar–*H*), 7.30–7.25 (m, 4H, Ar–*H*), 6.85–6.79 (m, 20H, Ar–*H*), 3.79–3.76 (t, 16H, O–C*H*$_2$), 3.16–3.14 (t, 16H, N–C*H*$_2$), 2.48 (s, 12H, C*H*$_3$). ^{13}C-NMR (δ in ppm, $CDCl_3$): 150.48, 147.58, 146.58, 143.78, 143.33, 140.56, 137.68, 136.30, 132.96, 130.29, 129.87, 129.74, 128.11, 124.63, 120.84, 112.16, 105.82, 102.30, 100.97, 66.85–66.77–66.56–65.83 (O–*C*H$_2$), 48.94–48.54–48.42 (N–*C*H$_2$), 22.68–22.59–21.70–21.52–20.81 (Ar–*C*H$_3$). UV-vis ($CHCl_3$), λ_{max}, nm (logε): 350 (4.60), 617 (4.28) and 684 (4.99). MALDI-TOF MS *m/z*: calculated: 1899.52; found: 1899.22 $[M]^+$.

2.4.3.4. Non-peripherally phthalocyaninato magnesium (II) (8). Color: Light green. Yield: 30.0 mg (29.8%), m.p. >300 °C. Elemental analysis: Calc. (%) for $C_{100}H_{88}N_{16}O_{12}S_4Mg$: C, 64.63; H, 4.77; N, 12.06; S, 6.90. Found (%): C, 64.18; H, 4.51; N, 11.76; S, 6.63. FT-IR, υ_{max} (cm^{-1}): 3044 (Aromatic C–H), 2956–2917–2894 (CH_3), 1606, 1509, 1483, 1332–1159 (SO_2-tosyl group), 1234, 1119, 1084, 926, 813, 752, 661. ^{1}H-NMR (δ in ppm, $CDCl_3$): 7.75–7.53 (m, 22H, Ar–*H*), 7.31–7.25 (m, 4H, Ar–*H*), 6.91–6.78 (m, 18H, Ar–*H*), 3.89–3.82 (t, 16H, O–C*H*$_2$), 3.18–3.15 (t, 16H, N–C*H*$_2$), 2.46 (s, 12H, C*H*$_3$). ^{13}C-NMR (δ in ppm, $CDCl_3$): 150.63, 148.82, 148.24, 144.22, 143.76, 142.93, 139.56,

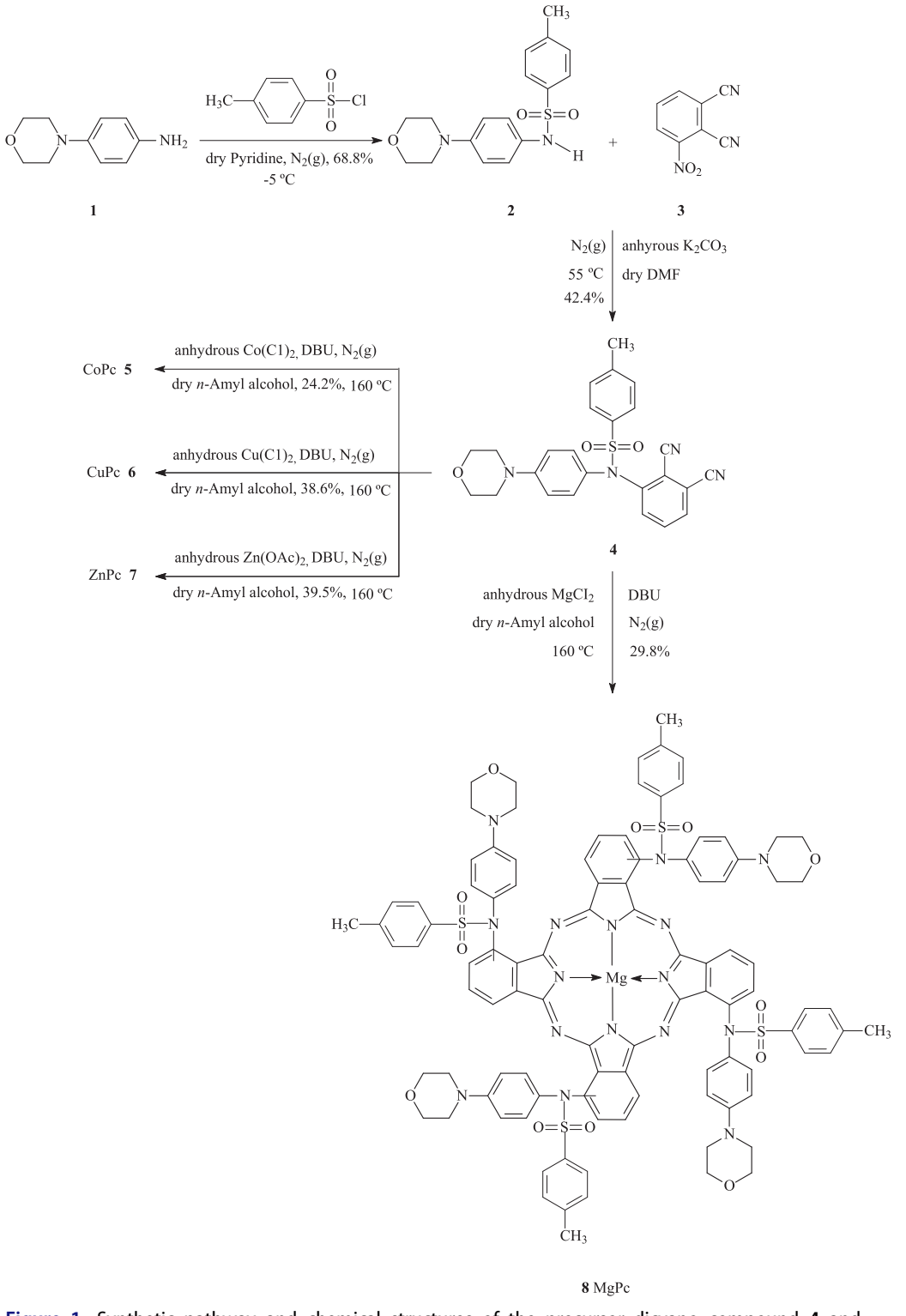

Figure 1. Synthetic pathway and chemical structures of the precursor dicyano compound **4** and metallated phthalocyanines **5**–**8**.

139.44, 137.62, 132.91, 132.62, 130.41, 129.79, 129.71, 128.02, 126.19, 123.37, 104.86, 103.63, 66.74–65.83 (O–CH_2), 48.67 (N–CH_2), 21.68 (Ar–CH_3). UV-vis ($CHC1_3$), λ_{max}, nm (logε): 355 (4.56), 619 (4.27) and 686 (5.00). MALDI–TOF MS *m/z*: calculated: 1858.43; found: 1858.13 $[M]^+$.

3. Results and discussion

3.1. Syntheses and structural verification

The synthetic procedures of newly synthesized tetra-substituted Co^{II} (**5**), Cu^{II} (**6**), Zn^{II} (**7**) and Mg^{II} (**8**) phthalocyanines fused 4-methyl-*N*-(4-morpholinophenyl)benzenesulfonamide units at their non-peripheral positions are illustrated in Figure 1. In this work, we obtained new organo-soluble metallated phthalocyanines which exhibited good solubility in dichloromethane (DCM), chloroform ($CHCl_3$), *N,N*-dimethylformamide (DMF), tetrahydrofuran (THF), ethyl acetate (EtOAc), and dimethylsulfoxide (DMSO) because of the substitution of 4-methyl-*N*-(4-morpholinophenyl)benzenesulfonamide units at non-peripheral sites of phthalocyanine core. To verify the structural characterization, we benefited from some spectroscopic techniques, including MALDI-TOF mass spectral data (Dithranol (DIT) for **7** and **8** and 2,5-dihydroxybenzoic acid (DHB) for **5** and **6** were used as the matrixes), UV-vis and FT-IR (ATR sampling accessory technique), ^{1}H-NMR and ^{13}C-NMR along with elemental analysis.

Starting from 4-morpholinoaniline (**1**), we obtained the tosylated compound **2**, 4-methyl-*N*-(4-morpholinophenyl)benzenesulfonamide, with 68.8% yield by adaptation of the tosylation reaction according to literature [36]. The proton NMR signal associated with the NH_2 group of **1** vanished and a new proton NMR resonance peak belonging to the N–H functionality was observed as a singlet signal integrating one proton at $\delta = 8.88$ ppm for **2** after the tosylation reaction achieved. The other ^{1}H-NMR peaks of **2** were resonated at 7.61–7.59 (Tosyl, Ar–*H*), 7.22–7.20 (Tosyl, Ar–*H*), 7.01–6.97 (Ar–*H*), 6.83–6.79 (Ar–*H*), 3.88–3.86 (O–C*H*$_2$), 3.13–3.11 (N–C*H*$_2$) and 2.38 ppm (C*H*$_3$). The carbon atom peaks belonging to the aromatic rings resonated at 148.70, 148.43, 132.96, 129.01, 126.10, 110.52, 107.91, 107.39, 106.19 and 105.91 ppm in the ^{13}C-NMR spectrum of **2**. Other carbon atom resonances of **2** were observed at 67.17–66.62–64.93 (O–CH_2), 50.12–49.83–49.65 (N–CH_2) and 22.31–21.59–20.59 ppm (Ar–CH_3) in the ^{13}C-NMR spectrum. Another indication that the tosylation reaction plainly succeeded is the evanescence of the primary amine (NH_2) vibration of **1** and the existence of new vibrational signals of **2** related to the tosyl group at $\upsilon = 1336$ and 1158 cm^{-1} (SO_2-tosyl group) and secondary amine (N–H) functionality at $\upsilon = 3154$ and 1051 cm^{-1} in the FT-IR spectrum of **2**. Accompanied with slight changes, the rest of the infrared vibrations of **2** were similar to those of the starting compound **1**. The mass spectral data measured with the MALDI-TOF method and the molecular ion peak (MIP) of **2** was detected at *m/z* = 332.07 $[M]^+$ (Figure S1 in the Supplementary Material).

N-(2,3-Dicyanophenyl)-4-methyl-*N*-(4-morpholinophenyl)benzenesulfonamide, the new precursor phthalonitrile compound **4**, was obtained from the reaction of 4-methyl-*N*-(4-morpholinophenyl)benzenesulfonamide **2**, 3-nitrophtalonitrile **3** and anhydrous K_2CO_3 in the existence of dry DMF under an inert nitrogen atmosphere with 42.4% yield after the purification process. As the synthesis of targeted

phthalonitrile compound **4** was accomplished successfully from the reaction of tosylated derivative **2**, a new vibrational peak was detected at $\upsilon = 2233\,cm^{-1}$ belonging to the C≡N functional group instead of the vibration signals regarding the N–H functionality at $\upsilon = 3154$ and $1051\,cm^{-1}$ in the vibrational spectra of **2**, which was a good sign of the formation of phthalonitrile derivative **4**. One of the best indications of the achievement of base-catalyzed aromatic nitro-displacement reaction of 3-nitrophthalonitrile **3** in terms of NMR spectroscopy is to see C≡N resonance peak at 115.40 ppm in the ^{13}C-NMR spectrum of **4** and the disappearance of the singlet resonance signal of N–H proton, which was resonated at 8.88 ppm in the ^{1}H-NMR spectrum of **2** (Figure S2 in the Supplementary Material). Other FT-IR, ^{1}H-NMR and ^{13}C-NMR spectral data were similar to that of the tosylated compound **2** with slight changes. In the MALDI-TOF spectrum of **4**, MIP was detected at $m/z = 458.17$ $[M]^+$ (Figure S1 in the Supplementary Material).

We synthesized the targeted new metallated Pcs [Co^{II} (**5**), Cu^{II} (**6**), Zn^{II} (**7**) and Mg^{II} (**8**)] through the cyclotetramerization reaction of the precursor dicyano compound **4** with $CoC1_2$ for **5**, $CuC1_2$ for **6**, $Zn(OAc)_2$ for **7** and $MgC1_2$ for **8** in dry *n*-amyl alcohol and the catalytic effect of the strong base DBU at 160 °C for 17 h under a $N_{2(g)}$ stream with moderate yields after the purifying column chromatography processes. In the case of new phthalocyaninato metal complexes **5**–**8**, the evanescence of the C≡N functionality at $2233\,cm^{-1}$ in the vibrational spectra of phthalonitrile derivative **4** is among the best structural corroboration methods. Likewise, the resonance peak associated with C≡N groups at 115.40 ppm in the ^{13}C-NMR spectrum of **4** was also evanesced after the syntheses of the corresponding metal complexes as well. Since **5** and **6** have paramagnetic transition metal ions inside the center of their phthalocyanine core, their NMR measurements precluded. Except for some little chemical shifts, ^{1}H-NMR and ^{13}C-NMR spectra of **7** and **8** were similar to that of **4**. According to the MALDI-TOF mass spectral data, the parent molecular ion peaks were detected at $m/z = 1893.23$ $[M]^+$ for **5**, 1897.11 $[M]^+$ for **6**, 1899.22 $[M]^+$ for **7** and 1858.13 $[M]^+$ for **8** (Figure S3 in the Supplementary Material for **7** and **8**). Coupled with synthesis procedures, all spectral data including elemental analysis results are in good harmony with the suggested chemical compounds.

3.2. Electronic absorption spectra

As remarked previously that the cyclotetramerization reaction of the dicyano compound **4** succeeded and metallated phthalocyanines were obtained, the electronic absorption spectra of MPcs **5**–**8** give us some considerable evidence in addition to the spectroscopic data summarized above. To put it another way, the characteristic B-(Soret) and Q-bands in UV-vis spectra (measured at room temperature in chloroform at 1×10^{-5} M concentration) of MPcs **5**–**8** were easily identified at first glance. The absorptions related with B-band were seen at 327 nm ($\log\varepsilon = 4.84$) for **5**, 344 nm ($\log\varepsilon = 4.71$) for **6**, 350 nm ($\log\varepsilon = 4.60$) for **7** and 355 nm ($\log\varepsilon = 4.56$) for **8**. In addition to intense and sharp Q-band absorptions, shoulders were observed at lower wavelengths as well. The shoulders accompanied with narrow and intense Q-bands can be attributable to the charge-transfer transitions from ligand-to-metal and/or metal-to-

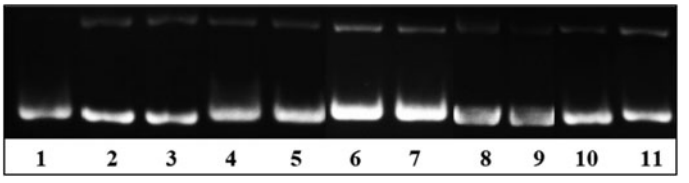

Figure 2. Supercoiled pBR322 plasmid DNA properties of CoPc (**5**). Lane 1: DNA control; lane 2: **5** (12.5 μM); lane 3: **5** (25 μM); lane 4: **5** (12.5 μM) + irradiation; lane 5: **5** (25 μM) + irradiation; lane 6: **5** (12.5 μM) + H_2O_2 (0.4 M); lane 7: **5** (25 μM) + H_2O_2 (0.4 M); lane 8: **5** (12.5 μM) + H_2O_2 (0.4 M) + irradiation; lane 9: **5** (25 μM) + H_2O_2 (0.4 M) + irradiation; lane 10: H_2O_2 (0.4 M); lane 11: H_2O_2 (0.4 M) + irradiation.

ligand [36]. The specific Q-bands were seen at 607 nm ($\log\varepsilon = 4.42$) and 671 nm ($\log\varepsilon = 5.01$) for **5**, 612 nm ($\log\varepsilon = 4.35$) and 680 nm ($\log\varepsilon = 5.01$) for **6**, 617 nm ($\log\varepsilon = 4.28$) and 684 nm ($\log\varepsilon = 4.99$) for **7** and 619 nm ($\log\varepsilon = 4.27$) and 686 nm ($\log\varepsilon = 5.00$) for **8**. In light of the UV-vis spectra of the studied phthalocyanine metal complexes **5**–**8**, the single and intense Q-bands exhibited that all measured MPcs **5**–**8** under the circumstances summarized above had D_{4h} point group with monomeric species (no aggregation) of metallophthalocyanines [3, 37].

3.3. DNA-cleavage studies

The hydrolytic, oxidative and photo supercoiled (SC) pBR322 plasmid DNA cleavage features of the new non-peripherally tetra-substituted organo-soluble Co^{II} **5**, Cu^{II} **6**, Zn^{II} **7** and Mg^{II} **8** phthalocyanines were investigated using agarose gel electrophoresis. It is well-known that when single-strand cleavage of SC forms nicked circular (NC) form, double-strand cleavage of SC occurs linear form (LN) that moves between SC and NC [38]. The results of hydrolytic, oxidative and photo DNA cleavage properties of **5**–**8** at 12.5 and 25 μM are presented in Figures 2–5 and analyzed using Image Lab Version 4.0.1 Software. SC showed single-band in the absence of compounds or agent [hydrogen peroxide (H_2O_2)] as a negative control, as shown in Figures 2–5 (lane 1). Figure 2 demonstrated that **5** did not show any considerable cleavage effects against plasmid DNA under our conditions. In Figure 3, **6** was almost inactive in the dark (lanes 2 and 3) but the compound had oxidative photocleavage activities with irradiation at 700 nm (17.5 mW/cm^2, 15 min) in the presence of H_2O_2 showing the conversion of SC to NC and LN (lanes 8 and 9) owing to reactive oxygen species which have been generated by phthalocyanines under irradiation. It is well-known that oxidative activator such as H_2O_2 is important to begin the cleavage process. NC (19.90%) and LN (4.40%) were observed and SC (75.70%) diminished on increasing concentrations of **7** at 25 μM in the presence of H_2O_2 and irradiation at 700 nm (17.5 mW/cm^2, 15 min) (Figure 4, lane 9). In Figure 5, **8** had no hydrolytic, oxidative and photo activities against SC. Barut et al. reported that water-soluble morpholine substituted Zn(II) phthalocyanine had significant cleavage properties at 25, 50 and 100 μM [39]. In addition, Sankarganesh et al. reported that Cu(II) and Zn(II) complexes with 4-(1-(4-morpholinophenyl)ethylideneamino)pyrimidine-5-carbonitrile) had moderate cleavage activities against calf-thymus DNA [40].

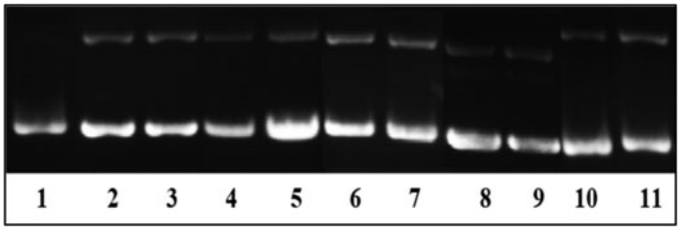

Figure 3. Supercoiled pBR322 plasmid DNA cleavage properties of CuPc (**6**). Lane 1: DNA control; lane 2: **6** (12.5 μM); lane 3: **6** (25 μM); lane 4: **6** (12.5 μM) + irradiation; lane 5: **6** (25 μM) + irradiation; lane 6: **6** (12.5 μM) + H_2O_2 (0.4 M); lane 7: **6** (25 μM) + H_2O_2 (0.4 M); lane 8: **6** (12.5 μM) + H_2O_2 (0.4 M) + irradiation; lane 9: **6** (25 μM) + H_2O_2 (0.4 M) + irradiation; lane 10: H_2O_2 (0.4 M); lane 11: H_2O_2 (0.4 M) + irradiation.

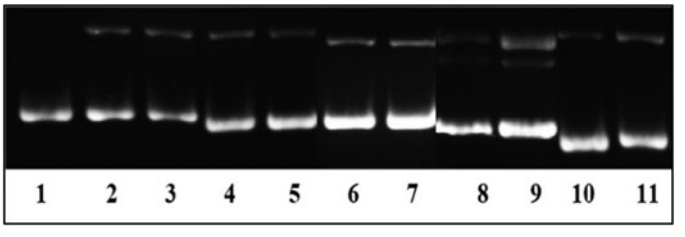

Figure 4. Supercoiled pBR322 plasmid DNA cleavage properties of ZnPc (**7**). Lane 1: DNA control; lane 2: **7** (12.5 μM); lane 3: **7** (25 μM); lane 4: **7** (12.5 μM) + irradiation; lane 5: **7** (25 μM) + irradiation; lane 6: **7** (12.5 μM) + H_2O_2 (0.4 M); lane 7: **7** (25 μM) + H_2O_2 (0.4 M); lane 8: **7** (12.5 μM) + H_2O_2 (0.4 M) + irradiation; lane 9: **7** (25 μM) + H_2O_2 (0.4 M) + irradiation; lane 10: H_2O_2 (0.4 M); lane 11: H_2O_2 (0.4 M) + irradiation.

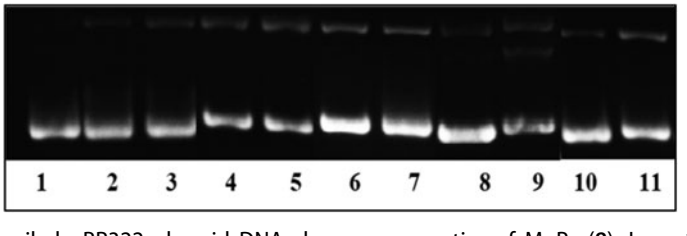

Figure 5. Supercoiled pBR322 plasmid DNA cleavage properties of MgPc (**8**). Lane 1: DNA control; lane 2: **8** (12.5 μM); lane 3: **8** (25 μM); lane 4: **8** (12.5 μM) + irradiation; lane 5: **5** (25 μM) + irradiation; lane 6: **8** (12.5 μM) + H_2O_2 (0.4 M); lane 7: **8** (25 μM) + H_2O_2 (0.4 M); lane 8: **8** (12.5 μM) + H_2O_2 (0.4 M) + irradiation; lane 9: **8** (25 μM) + H_2O_2 (0.4 M) + irradiation; lane 10: H_2O_2 (0.4 M); lane 11: H_2O_2 (0.4 M) + irradiation.

3.4. DPPH radical scavenging assay

DPPH assay is one of the routinely and easy colorimetric methods to determine radical scavenging potential of compounds [41]. The results of DPPH radical scavenging properties of **5**–**8** at 12.5, 25, 50 and 100 μM are depicted in Table 1. Gallic acid (GA) was used as positive control. As shown in Table 1, **5** displayed the highest radical scavenging activities among the tested compounds at all concentrations. Compound **5** ranged from 85.35 ± 2.45% (12.5 μM) to 95.38 ± 1.44% (100 μM). At 12.5 and 25 μM, **5** showed higher antioxidant activity than GA as a positive control. The other compounds (**6**–**8**)

Table 1. Radical-scavenging activity on DPPH radicals (%) of **5**–**8**.

μM	5	6	7	8	GA
12.5	85.35 ± 2.45	13.98 ± 0.88	15.96 ± 1.37	5.01 ± 0.34	60.38 ± 0.22
25	90.10 ± 2.40	15.30 ± 2.49	26.25 ± 2.29	18.86 ± 1.93	80.03 ± 0.35
50	94.98 ± 1.04	23.88 ± 2.74	34.96 ± 2.66	39.31 ± 3.91	96.93 ± 1.25
100	95.38 ± 1.44	34.70 ± 3.92	41.42 ± 3.91	53.03 ± 4.22	98.93 ± 1.50

had moderate radical scavenging activities from 5.01 ± 0.34% to 53.03 ± 4.22%. Fadda et al. reported that new Pcs carrying peripherally functionalized fused heterocyclic compounds showed DPPH radical scavenging activities with IC_{50} values of 0.098–6.011 mM [42]. Aydın et al. reported that IC_{50} values of tetra-substituted Zn(II) and Co(II) phthalocyanines bearing (4-(methylthio)phenylthio) were determined as 0.1 ± 0.02 and 0.09 ± 0.03 mg/mL [43].

4. Conclusion

Herein, we reported the synthesis processes and structural characterization of the new non-peripheral tetra-substituted organo-soluble Co^{II} (**5**), Cu^{II} (**6**), $Zn^{(II)}$ (**7**) and $Mg^{(II)}$ (**8**) phthalocyanine complexes carrying four 4-methyl-*N*-(4-morpholinophenyl)benzenesulfonamide units. The structural characterization of the newly synthesized molecules was elucidated by spectroscopic techniques comprising elemental analysis, MALDI-TOF mass spectral data, FT-IR, ^{1}H-NMR (for **2**, **4**, **7** and **8**), UV-vis (for **5**–**8**) and ^{13}C-NMR (for **2**, **4**, **7** and **8**). The hydrolytic, oxidative and photo DNA-cleavage effects of the products were investigated by agarose gel electrophoresis. Compound **7** indicated oxidative photocleavage activity in the presence of H_2O_2, indicating the conversion of supercoiled pBR322 plasmid DNA to nicked circular form (19.90%) and linear form (4.40%). In addition, DPPH-radical scavenging percentages of the compounds were determined using colorimetric methods and **5** displayed the highest radical scavenging activity among the tested compounds. The DPPH radical scavenging percentages of **5** ranged from 85.35 ± 2.45% (12.5 μM) to 95.38 ± 1.44% (100 μM). Compounds **5**–**8** synthesized under the framework of this study are favorable for further research since the broad range of pharmaceutical and biological activities of morpholine-based compounds.

Disclosure statement

No potential conflict of interest was reported by the authors.

References

[1] B. Ertem, G. Sarkı, H. Yalazan, Z. Bıyıklıoğlu, H. Kantekin. *Inorg. Chim. Acta*, **462**, 123 (2017).
[2] B. Ertem, H. Yalazan, Ö. Güngör, G. Sarki, M. Durmuş, E.T. Saka, H. Kantekin. *J. Lumin.*, **204**, 464 (2018).
[3] H. Kantekin, H. Yalazan, N. Kahriman, B. Ertem, V. Serdaroğlu, M. Pişkin, M. Durmuş. *J. Photochem. Photobiol. A Chem.*, **361**, 1 (2018).
[4] H. Kantekin, E.T. Saka, B. Ertem, M.N. Mısır, H. Yalazan, G. Sarkı. *J. Coord. Chem.*, **71**, 164 (2018).

[5] H. Son, M.H. Yang, A.K. Mutyala, D.W. Chang, J.S. Park. *Dyes Pigm.*, **162**, 662 (2019).
[6] C.G. Claessens, U. Hahn, T. Torres. *Chem. Rec.*, **8**, 75 (2008).
[7] G.K. Karaoğlan, G. Gümrükçü, A. Koca, A. Gül. *Dyes Pigm.*, **88**, 247 (2011).
[8] A.K. Mutyala, S.-M. Hong, J.W. Namgoong, J.P. Kim, J.S. Park. *Dyes Pigm.*, **142**, 237 (2017).
[9] G. de la Torre, G. Bottari, M. Sekita, A. Hausmann, D.M. Guldi, T. Torres. *Chem. Soc. Rev.*, **42**, 8049 (2013).
[10] F.I. Bohrer, C.N. Colesniuc, J. Park, M.E. Ruidiaz, I.K. Schuller, A.C. Kummel, W.C. Trogler. *J. Am. Chem. Soc.*, **131**, 478 (2009).
[11] T. Goslinski, T. Osmalek, K. Konopka, M. Wierzchowski, P. Fita, J. Mielcarek. *Polyhedron*, **30**, 1538 (2011).
[12] E. Güzel, G.Y. Atmaca, A. Erdoğmuş, M.B. Koçak. *J. Coord. Chem.*, **70**, 2659 (2017).
[13] E. Güzel, A. Atsay, S. Nalbantoglu, N. Şaki, A.L. Dogan, A. Gül, M.B. Koçak. *Dyes Pigm.*, **97**, 238 (2013).
[14] E. Güzel, A. Günsel, B. Tüzün, G.Y. Atmaca, A.T. Bilgiçli, A. Erdoğmuş, M.N. Yarasir. *Polyhedron*, **158**, 316 (2019).
[15] T.V. Basova, R.G. Parkhomenko, M. Polyakov, A.G. Gürek, D. Atilla, F. Yuksel, E.I. Ryabchikova, B.Y. Kadem, A.K. Hassan. *Dyes Pigm.*, **125**, 266 (2016).
[16] B. Brozek-Pluska, M. Orlikowski, H. Abramczyk. Phthalocyanines: From dyes to photosensitizers in diagnostics and treatment of cancer. Spectroscopy and Raman imaging studies of phthalocyanines in human breast tissues In *Handbook of Porphyrin Science: With Applications to Chemistry, Physics, Materials Science, Engineering, Biology and Medicine, World Scientific* (2016).
[17] M. Soylu, R. Ocaya, H. Tuncer, A.A. Al-Ghamdi, A. Dere, D.C. Sari, F. Yakuphanoglu. *Microelectron. Eng.*, **154**, 53 (2016).
[18] Y. Çimen, E. Ermiş, F. Dumludağ, A.R. Özkaya, B. Salih, Ö. Bekaroğlu. *Sens. Actuators B*, **202**, 1137 (2014).
[19] D.O. Oluwole, S.M. Ngxeke, J. Britton, T. Nyokong. *J. Photochem. Photobiol. A Chem.*, **347**, 146 (2017).
[20] D. Arıcan, A. Erdoğmuş, A. Koca. *Thin Solid Films*, **550**, 669 (2014).
[21] T. Kawata, Y. Chino, N. Kobayashi, M. Kimura. *Langmuir*, **34**, 7294 (2018).
[22] T.S. Harish, P. Viswanath. *Thin Solid Films*, **598**, 170 (2016).
[23] C. Kantar, V. Mavi, N. Baltaş, F. İslamoğlu, S. Şaşmaz. *J. Mol. Struct.*, **1122**, 88 (2016).
[24] O.J. Achadu, T. Nyokong. *Dyes Pigm.*, **145**, 189 (2017).
[25] A. Shaabani, S.E. Hooshmand, R. Afshari, S. Shaabani, V. Ghasemi, M. Atharnezhad, M. Akbari. *J. Solid State Chem.*, **258**, 536 (2018).
[26] G. Löbbert. In *Ullmann's Encyclopedia of Industrial Chemistry*, Wiley-VCH Verlag GmbH & Co., KGaA, Weinheim (2000).
[27] M.J. Naim, O. Alam, M.J. Alam, P. Alam, N. Shrivastava. *J. Pharm. Bioall. Sci.*, **3**, 40 (2015).
[28] P. Panneerselvam, R.V. Pradeepchandran, S.K. Sreedhar. *Indian J. Pharm. Sci.*, **65**, 268 (2003).
[29] G.R. Brown, A.J. Foubister, D. Stribling. *J. Chem. Soc. Perkin Trans.*, **1**, 547 (1987).
[30] A.H. El-Masry, H.H. Fahmy, S.H.A. Abdelwahed. *Molecules*, **5**, 1429 (2000).
[31] V. Duhalde, B. Lahille, F. Camou, S. Pédeboscq, J.-P. Pometan. *Pathol. Biol.*, **55**, 478 (2007).
[32] C. Marcireau, M. Guilloton, F. Karst. *Antimicrob. Agents Chemother.*, **34**, 989 (1990).
[33] S.P. Sawargave, A.S. Kudale, J.V. Deore, D.S. Bhosale, J.M. Divse, S.P. Chavan, H.B. Borate. *Tetrahedron Lett.*, **52**, 5491 (2011).
[34] Z. Biyiklioglu, B. Barut, A. Özel. *Dyes Pigm.*, **148**, 417 (2018).
[35] R.D. George, A.W. Snow. *J. Heterocycl. Chem.*, **32**, 495 (1995).
[36] M. Koçak, A.İ. Okur, Ö. Bekaroğlu. *J. Chem. Soc. Dalton Trans.*, **323**, (1994).
[37] A. Bilgin, B. Ertem, Y. Gök. *Eur. J. Inorg. Chem.*, **2007**, 1703 (2007).
[38] C. Gökçe, N. Dilek, R. Gup. *Inorg. Chim. Acta*, **432**, 213 (2015).
[39] B. Barut, Ü. Demirbaş, A. Özel, H. Kantekin. *Int. J. Biol. Macromol.*, **105**, 499 (2017).
[40] M. Sankarganesh, J. Rajesh, G.G.V. Kumar, M. Vadivel, L. Mitu, R.S. Kumar, J.D. Raja. *J. Saudi Chem. Soc.*, **22**, 416 (2018).

[41] K. Mishra, H. Ojha, N.K. Chaudhury. *Food Chem.*, **130**, 1036 (2012).
[42] A.A. Fadda, R.E. El-Mekawy, N.N. Soliman, A.M. Allam, M.T. Abdelaal. *Dyes Pigm.*, **155**, 300 (2018).
[43] M. Aydın, E.H. Alıcı, A.T. Bilgiçli, M.N. Yarasir, G. Arabacı. *Inorg. Chim. Acta*, **464**, 1 (2017).